Orbital: The Electronic Journal of Chemistry
journal homepage: www.orbital.ufms.br
e-ISSN 1984-6428

| Vol 12 | | No. 3 | | July-September 2020 |

FULL PAPER

Microwave Assisted Synthesis of Chromium Substituted Nickel Ferrite Spinel for Oxygen Evolution Reaction

Basant Lal* **and Pankaj Kumar Rastogi**

Department of Chemistry, Institute of Applied Science and Humanities, GLA University, Mathura, U. P., India – 281 406.

Article history: Received: 28 May 2020; revised: 26 July 2020; accepted: 01 August 2020. Available online: 30 September 2020. DOI: http://dx.doi.org/10.17807/orbital.v12i3.1507

Abstract:

Herein, a simple microwave assisted combustion approach is utilized for the synthesis of nano-sized Cr substituted Ni ferrites ($NiCr_xFe_{2-x}O_4$). The as obtained materials were further sintered at 450°C in air and then utilized for physicochemical and electrochemical characterizations. X-ray diffraction (XRD) patterns showing sharp peaks confirmed the formation of single phase cubic spinel structure. TEM image reveals the formation of nanocrystalline particles having size in range of 10-20 nm. Further, the electrocatalytic oxygen evolution reaction (OER) of as-synthesized materials was studied by linear sweep voltammetry in alkaline solution. The OER results showed that co-substitution of Cr in $NiFe_2O_4$ matrix improved the electrocatalytic activity of the oxides towards OER. The $NiCr_{0.5}Fe_{1.5}O_4$ shows the best OER performance in 1.0 M KOH solution. It achieved a low overpotential of about 320 mV at 10 mA/cm^2 current density, which is comparable to other reported electrocatalysts. Tafel parameters and order of reaction were also in close agreements with literature values.

Keywords: spinel; nickel ferrite; microwave; electrocatalysis; oxygen evolution reaction

1. Introduction

Water electrolysis is considered as one of the best, proficient and clean methods for production of hydrogen, and could solve the energy crisis and environmental pollution [1-3]. However, it has been immensely hampered by the two sluggish half reactions namely hydrogen evolution reaction (HER) and oxygen evolution reaction (OER). Among these two reactions, the OER has more sluggish kinetics due to the involvement of four electron transfer process [4-6] and essentially requires noble metal oxide (IrO_2 and RuO_2) based state-of-the-art electrocatalysts to speed up the reaction kinetics of OER. However, their high cost and rare occurrence is significantly reduced down the large-scale practical applications [5, 6]. Therefore, to address this problem, numerous low cost and earth-abundant non-precious metal based oxides were developed for effectively catalyzed the sluggish OER kinetics and attracted much attention due to their and abundant catalytic active sites [4, 5].

Spinel-type nickel ferrites nano particles based binary/ternary metal oxide oxide materials with molecular formula MFe_2O_4 (M = bivalent metal ions e.g. Mg, Mn, Co, Ni, Cu, Zn etc.) are considered as vital materials for several applications such as magnetic storage devices, electrochemical energy storage (batteries and electrochemical capacitors), photocatalysis, electrocatalysis and in biosensors [7-13]. These large applications of nickel ferrite nano-particles based materials are due to its excellent chemical, physical and magnetic properties than bulk materials. Several methods such as co-precipitation [14], sol–gel [15], microemulsion [16], hydrothermal [17], microwave assisted combustion [18], etc. have been reported for the synthesis of nickel ferrite nanoparticles with various particle sizes and morphologies. Among these methods, the microwave assisted combustion methods have several advantages

*Corresponding author. E-mail: basant.lal@gla.ac.in

over other methods like significant reduction in reaction time and energy costs, fast heating, and formation of homogeneous products, shape control, high yield and high purity. Microwave-assisted combustion approach was also carried out to synthesize manganese oxides, α-Fe_2O_3 nanoparticles and nickel ferrite [19-21].

Due to presence of multiple oxidation states transition metals in same lattice, $NiFe_2O_4$ based materials are also got special interest in electrocatalysis. Several investigations have been carried to developed transition metal oxides with spinel and perovskite type structures to improve electrocatalytic activities for OER in alkaline solutions [12-19]. Several efforts have been made to enhance the electrocatalytic activities either synthesized oxide catalysts at low temperature method [20-23] or substitution of other metal ions in oxide matrix [24-29]. For example, Singh et al studied the effect of partial substitution of Cr in nickel ferrites for oxygen evolution in alkaline solutions and observed that significant improvement in electrocatalytic OER activity [30].

Thus, the present investigations performed with the aim to study the effects of substitution of iron by chromium in nickel ferrite obtained by microwave assisted combustion method on their physicochemical and electrocatalytic properties for OER in alkaline solutions.The results revealed that Cr substitutions on nickel ferrite ($NiCr_{0.5}Fe_{1.5}O_4$) are superior OER catalytic activity than that of nickel ferrite alone which clearly suggests that enhancement of catalytic active sites.

2.Results and Discussion

2.1 X-ray Diffraction (XRD) Analysis

X-ray diffraction study was carried out in order to check the phase purity and crystalline phase of as-synthesized materials. Figure 1 shows the diffraction patterns of the synthesized oxides materials recorded between 2θ = 20 to 2θ = 70°. The sharp peaks in XRD spectra clearly indicated that the formation of pure spinel phage with cubic cell geometry. The XRD pattern of the samples showed the reflection planes of (220), (311), (222), (400), (422), (511) and (440) planes at 30.12°, 35.54°, 36.80°, 43.05°, 53.60°, 57.18° and 62.78° respectively, which confirm the presence of single-phase $NiFe_2O_4$ with a face centred cubic structure. The observed peaks are well matched with peaks of $NiFe_2O_4$ given in JCPDS card No. 74-2081. No additional peaks of γ-Fe_2O_3 and other impurities in spectra confirm purity of oxides. However, the XRD pattern shows a slight shift in the position of the peaks to smaller 2θ value with increasing concentrations of chromium. The lattice cell dimension (a) is also calculated based on the respective parameters (hkl) of the materials which is in range of 8.302 - 8.339 Å. Cr-substitutions in ferrite matrix causes slight reduction in value of 'a' this is due to smaller size of Cr^{3+} than that of Fe^{3+} ions and suggesting that Cr are probably incorporated in the available octahedral voids. The crystallite size of the oxide was estimated from XRD patterns by using Scherrer`s formula, $S = \frac{0.9\lambda}{B\cos\theta}$ where S is the size of grain, λ the wavelength of X-ray (1.5405Å), B the full width at half maxima of most intense peak. The unit cell parameters cell dimension (a), volume (V), crystallite density (d) and grain size (s) are shown in Table 1. The average grain size was found to be 21±2 nm [30, 31].

Table 1. Unit cell parameters of Cr-substituted nickel ferrites (FCC).

Sample	a (Å)	V $(Å)^3$	d $(gm\ (Å)^{-3})$	S (nm)
$NiFe_2O_4$	8.339	~580	3.234	~23
$NiCr_{0.5}Fe_{1.5}O_4$	8.302	~572	2.886	~19
$NiCr_{0.8}Fe_{1.2}O_4$	8.306	~573	2.648	~20

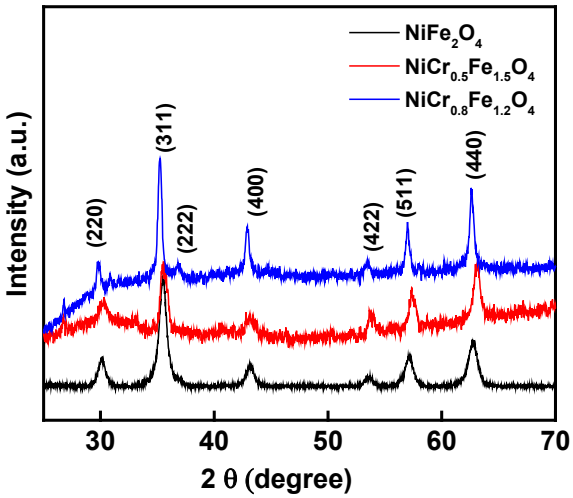

Figure 1. Powder XRD patterns of as synthesized $NiCr_xFe_{2-x}O_4$ nanoparticles sintered at 450°C for 5 h.

2.2 FT-IR studies

FT-IR spectra recorded in the region, 400 – 4000 cm^{-1} (Figure 2) also support the formation of spinel-type oxide. As depicted, FT-IR spectra of $NiCr_xFe_{2-x}O_4$ exhibited two main absorption bands, one of high intensity at ~ 580 cm^{-1} and another of low intensity at ~ 450 cm^{-1}. These absorption bands are corresponding to $M_{oh} \leftrightarrow O$ and $M_{Td} \leftrightarrow O$ stretching vibrations, respectively and clearly suggesting the formation of single phasic spinel structure having two sub-lattices, tetrahedral (A) and octahedral (B) sites. The absorption band observed at ~1120 cm^{-1} is due to $Fe^{3+} \leftrightarrow O^{2-}$ stretching vibration at tetrahedral void. The IR spectra also indicated the presence of water moiety in oxide by two additional bands ~1632 cm^{-1} and 3400 cm^{-1} are attributed to water molecule absorbs on surface of $NiFe_2O_4$ crystal lattice [31].

2.3 Morphology of oxide powder

The SEM and TEM micrographs of $NiCr_{0.5}Fe_{1.5}O_4$ sample are shown in the Figure 3 (a & b), respectively. From the SEM images, it is revealed that oxide particles have spherical shape morphology. Some aggregates have also been observed in the morphology of $NiCr_{0.5}Fe_{1.5}O_4$ (Figure 1a) due to the magnetic attraction since the specific surface area (surface-to-volume ratio) is large resulting in a high surface energy. The TEM images (Figure 3b) of as-synthesized substituted Cr ferrite sample ($NiCr_{0.5}Fe_{1.5}O_4$) is further confirming that the particles are spherical shape with an average diameter of 10 to 20 nm, which is matching well with the crystallite size calculated from the XRD results.

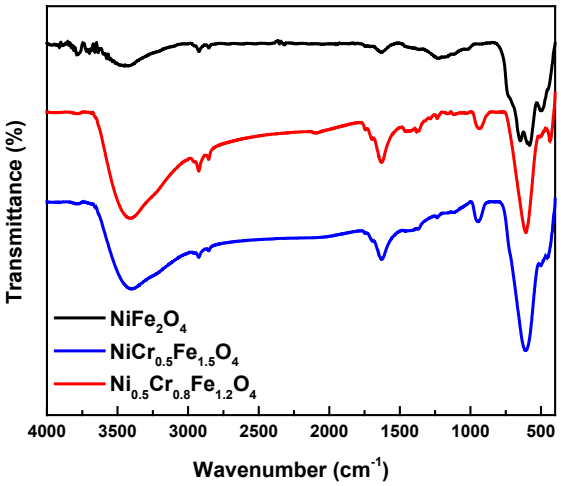

Figure 2. FT-IR spectrum of the as-synthesized $NiCr_xFe_{2-x}O_4$ nanoparticles.

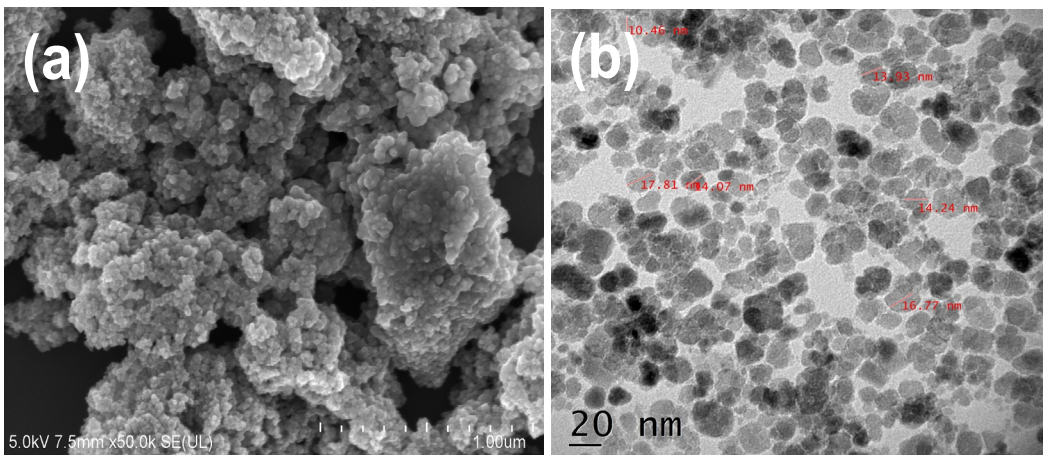

Figure 3. (a) Scanning electron and (b) transmission electron microscopic images of $NiCr_{0.5}Fe_{1.5}O_4$ nanoparticles.

2.4 Electrocatalytic oxygen evolution reaction

Further, the potential application of the as-synthesized chromium substituted ferrite materials were evaluated by measuring the electrocatalytic oxygen evolution reaction (OER) activity. The OER activities of each material were measured using linear sweep voltammetry (LSV) in 1.0 M KOH solution at a scan rate of 10 mV s^{-1}

at 25^{0}C. Each catalyst was drop casted onto the surface of glassy-carbon electrodes and standard three electrodes system was employed for the measurements of polarization curves. Results for the OER activity with different compositions are shown in Figure 4 along with the commercially available benchmark IrO_2 catalyst under similar experimental condition. It can be seen from the polarization curve (Figure 4a) that, the only $NiFe_2O_4$ shows poor OER activity whereas the substitution of Cr in $NiFe_2O_4$ matrix shows the improved OER performance compare to only $NiFe_2O_4$. The un-substituted $NiFe_2O_4$ sample displays a high overpotential around 406 mV at 10 mA cm^{-2}. However, when some Fe^{3+} ions of inverse spinel structure is substituted by Cr^{3+} ions the OER performance of the material has been improved for OER activity. More interestingly, we found that the amount of Cr substitution has profound effect on OER activity which can be further controlled by changing the ratio of Cr and Fe. The $NiCr_{0.5}Fe_{1.5}O_4$ shows the best performance with overpotential around 320 mV at 10 mA cm^{-2} current density, whereas, further increase of chromium content in nickel ferrite ($NiCr_{0.8}Fe_{1.2}O_4$) significantly decreases the OER activity (360 mV at 10 mA cm^{-2}). Additionally, the OER activity of a commercial benchmark IrO_2 catalyst was also evaluated for comparison. As shown in Fig. 4a, the corresponding overpotential to reach 10 mA cm^{-2} is 300 mV, which is very close to the $NiCr_{0.5}Fe_{1.5}O_4$.

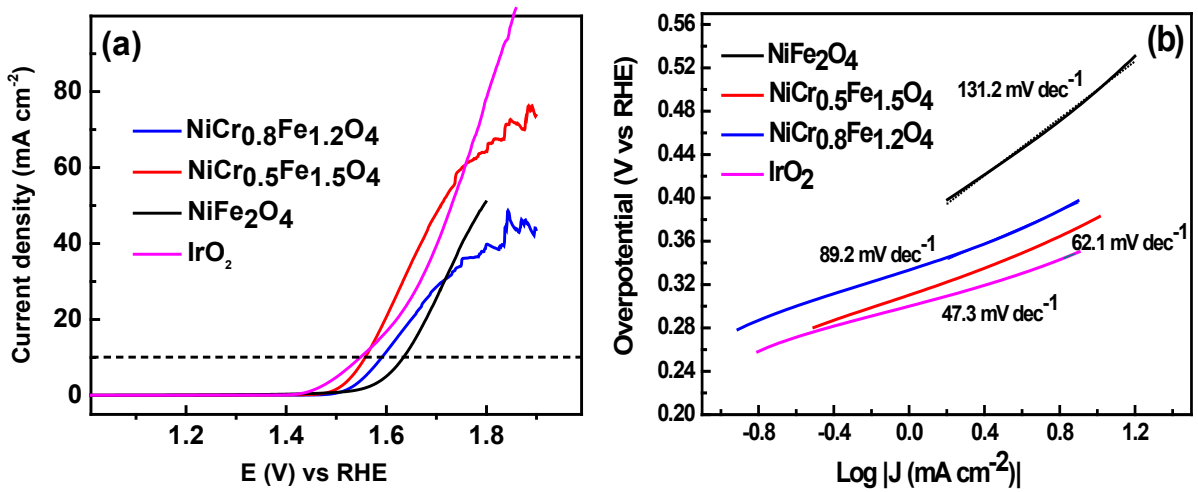

Figure 4. Oxygen evolution reaction performance as a function of electrode type in the presence of a 1 M KOH solution. (a) Polarization curves, and (b) corresponding Tafel plots.

The OER performances of the electrocatalysts with different composition of Cr are further evaluated in detail by the Tafel slope. The Tafel slope corresponding to polarization curves are shown in Figure 4b. A Tafel slope of 131.2 mV per decade is observed for $NiFe_2O_4$. In contrast, the substituted $NiCr_xFe_{2-x}O_4$ (x = 0.5, and 0.8) samples are substantially showing the better kinetics for OER activities. A greatly decreased Tafel slope of 62.1 mV per decade is observed for the $NiCr_{0.5}Fe_{1.5}O_4$. This observed value of Tafel slope is very much close to the benchmarked IrO_2 catalyst. In addition, a smaller Tafel slope of $NiCr_{0.5}Fe_{1.5}O_4$ is also very much comparable to other catalysts reported for OER activities [32], suggesting a more favourable OER catalytic kinetics. The high OER activity of a mixed cationic sub-lattice in the spinel structure of $NiCr_{0.5}Fe_{1.5}O_4$ is possibly due to the presence of Fe^{2+}, Fe^{3+}, Ni^{2+} and Cr^{3+} in spinel lattice which provide more catalytic active surface sites for breaking –O-H bond and enhanced electron transfer kinetics. The oxide electrodes followed the order of activity towards oxygen evolution reaction in 1 M KOH at 25^{0}C is $NiCr_{0.5}Fe_{1.5}O_4$> $NiCr_{0.8}Fe_{1.2}O_4$>$NiFe_2O_4$.

3. Material and Methods

3.1 Synthesis of materials

Cr-substituted nickel ferrites were prepared

by microwave assisted combustion method as reported previously [33] For the purpose, analytical reagent (AR) grade nickel nitrate hexahydrate ($Ni(NO_3)_2.6H_2O$), ferric nitrate nonahydrate ($Fe(NO_3)_2.9H_2O$), chromium nitrate nonahydrate ($Cr(NO_3)_3.9H_2O$) and urea ($CO(NH_2)_2$) were mixed in their stoichiometric ratios and heated in microwave oven at 800 watt for 10 minutes. At combustion point solution started burning with the evolution of large amount heat and brown dense fumes and whole material transformed into solid. The resultant product was crushed into fine powder form and further sintered in electrical furnace at 450^0C for 5 hours to gets the better cyrstallinity.

3.2. Characterizations

The crystalline structure and phase purity of the as-synthesized samples were analyzed by X-ray diffractometer (BRUKER D8 X-ray diffractometer) using Cu Kα radiation (λ= 0.15405 nm). The FT-IR spectra of the samples were recorded using PerkinElmer spectrometer (Spectrum two, UK). For the FT-IR measurements, the synthesized samples were mixed with spectroscopic grade KBr to form pellet and spectra were recorded in the range of 400-4000 cm^{-1}.The micrographs were obtained by scanning electron microscopy (JEOL SEM JSM-7200F) with an accelerating voltage of 20 kV. Transmission electron microscopy (TEM) images were obtained on TECNAI 20 G2 microscope operated at 200 kV.

3.3 Electrochemical measurements

All electrochemical investigations were performed (CHI-660C (CH instruments, USA)) in single compartment cell provided with three electrodes system consist of an oxide modified glassy carbon as a working electrode, platinum wire as a counter electrode and Ag/AgCl as a reference electrode. The modified electrodes were used as the working electrodes to investigate their electrocatalytic activities toward oxygen evolution reaction, each of which was cycled 30 times at a scan rate of 50 mV s^{-1} between 0 and 0.9 V vs. Ag/AgCl before data collection. All the potentials given in this paper are with respect to reversible hydrogen electrode (RHE). The potentials were changed to RHE scale by using the equation, $E_{RHE} = E_{Ag/AgCl} + 0.059\ pH + E^o_{Ag/AgCl}$, where, $E_{Ag/AgCl}$ is the experimentally measured potential *vs.* Ag/AgCl reference electrode. The standard electrode potential of Ag/AgCl reference electrode, $E^o_{Ag/AgCl}$ is used as 0.197 V. Cyclic voltammetry (CV) and linear sweep voltammetry (LSV) studies were carried out in 1.0 M KOH solution and the polarization curves are shown without iR compensation.

4.4 Preparation of electrodes

Typically, 3 mg of catalyst samples and 2 mg of acytene black powder were dispersed in 10 µL 5% Nafion and 500 µL ethanol using ultra sonication for at least 30 min to form the ink. Then, the 10 µL ink was dropped onto clean glassy carbon electrode surface and dried in air. Similarly, the benchmarked commercially available IrO_2 catalyst ink was prepared and drop casted on GC electrode. Prior to GC electrode modification, the electrode surface was thoroughly cleaned by rubbing it over the Buehlerfelt pad with alumina slurry followed by ultra-sonication in ethanol-water mixture solution.

4. Conclusions

A simple microwave assisted combustion method was economical and useful for preparation of the chromium substituted nickel ferrite ($NiCr_xFe_{2-x}O_4$) nanoparticles. The as-obtained materials were through characterized with XRD, FT-IR, SEM and TEM techniques which confirming the phase purity and morphological features of the prepared samples. Further, the electrocatalytic oxygen evolution performances shows that obtained chromium substituted nickel ferrite exhibits an improved OER performance with better kinetics. Thus developed method can be potential method to obtain $NiCr_xFe_{2-x}O_4$ nanoparticles for applications in energy conversion devices.

Acknowledgments

The authors express their sincere thanks to Dr. Piyush Kumar Sonkar, Department of Chemistry, MMV-BHU, Varanasi, India, for his help in XRD, FT-IR and electrochemical analysis.

References and Notes

[1] Zareyya, B.; Chekina, F.; Fathia, S. *Russ. J. Electrochem.* **2019**, *55*, 333. [Crossref]

[2] Pan, S.; Yu, J.; Zhang, Y.; Li B. *Mater. Lett.* **2020,** *262*, 127027. [Crossref]

[3] Fu, X.; Zhu, J.; Ao, B.; Lyu, X.; Chen, J. I*norg. Chem. Commun.* **2020,** *113*, 107802. [Crossref]

[4] Galini, M.; Salehi, M.; Behzad, M. *J. Nanostruct.* **2018,** *8*, 391. [Crossref]

[5] Raoof, J. B.; Chekin F.; Ehsani V. *Bull. Mater. Sci.* **2015,** *38*, 135. [Link]

[6] Yu, Y.; Liu, Y.; Ju, S.; Shen, X.; Ji, Z.; Kong, L.; Zhu. G. *Inorg. Chem. Commun.* **2020**, *111*, 107674. [Crossref]

[7] Pelini, M. P. *Adv. Funct. Mater.* **2001**, *5*, 323. [Crossref]

[8] Cheng, F. Y.; Su, C. H.; Yang, Y.; Yeh, C. S.; Tsa, C. Y.; Wu, C. L. *Biomaterials* **2005**, 26, 729. [Crossref]

[9] Song, Q.; Zhang, Z. J. *J. Am. Soc*. **2004**, *126*, 6164. [Crossref]

[10] Goldman, A. Modern Ferrite technology, Springer, New York, 2006.

[11] Niasari, M. S.; Davar, F.; Mahamoudi, T. *Polyhedron* **2009**, *28*, 1455. [Crossref]

[12] Rasiyah, P.; Tseung, A. C. C. *J. Electrochem. Soc.* **1982**, *103***,** 365. [Link]

[13] Boggio, R.; Carugati, A.; Trasatti, S. *J. Applied Electrochem.* **1987**, *17*, 828. [Link]

[14] Marsan, B.; Fradette, N.; Beaudoin, G. *J. Elelectrochem. Soc.* **1992**, *139*, 1889. [Link]

[15] Svegl, F.; Orel, B.; Grabec-Svegl, I.; Kancic, V. *Electrochim. Acta* **2000**, *45*, 4359. [Crossref]

[16] Tavares, A. C.; Cartaxo, M. A. M.; Da Silva Pereira, M. I.; Costa, F. M. *J. Electroanal. Chem.* **1999**, *464***,** 187. [Crossref]

[17] Bockris, J. O.; Otagawa, T. *J. Phys. Chem.* **1983**, *87*, 2960. [Crossref]

[18] Jain, A. N.; Tiwari, S. K.; Chartier, P.; Singh, R. N. *J. Chem. Soc. Faraday Trans.* **1995**, *91*, 1871. [Crossref]

[19] Singh, R. N.; Lal, B. *Int. J. Hydrogen Energy* **2002**, *27***,** 45. [Crossref]

[20] Singh, N. K.; Tiwari, S. K.; Anita, K. L.; Singh, R. N. *J. Chem. Soc. Faraday Trans.* **1996**, *92***,** 2397. [Crossref]

[21] El Baydi, M.; Poillerat, G.; Respringer, J. L.; Koenig, J.-F.; Chartier, P. *J. Solid State Chem.* **1994**, *109*, 281. [Crossref]

[22] El Baydi, M.; Tiwari, S. K.; Singh, R. N.; Rehspriger, J. L.; Chartier, P.; Koenig, J.-F.; Poillerat, G. *J. Solid State Chem.* **1995**, *116*, 157. [Crossref]

[23] Spinolo, G.; Ardizzone, S.; Trasatti, S. *J. Electroanal. Chem.* **1997**, *423*, 49. [Crossref]

[24] Nikolov, I.; Darkaou, R.; Zhecheva, E.; Stayanova, R.; Dimitrov, N.; Vitanov, T. *J. Elechtroanal Chem.* **1997**, *429*, 157. [Crossref]

[25] Fradetti, N.; Marsan, B. *J. Electrochem. Soc.* **1998**, *145*, 2320. [Link]

[26] Hu, C. C.; Lee, V. S.; Wen, T. C. *Mater. Chem. Physics* **1997**, *48*, 246. [Crossref]

[27] Genero, M. R.; Chialvo, D. E.; Chialvo, A. C. *Electrochim. Acta* **1993**, *38*, 2247. [Crossref]

[28] Lal, B.; Singh, N. K.; Samuel, S.; Singh, R. N. *J. New Mat. Electrochem. Systems* **1999**, *2*, 59.

[29] Singh, R. N.; Pandey, J. P.; Singh, N. K.; Lal, B.; Chartier, P.; Koenig, J. –F. *Electrochim. Acta* **2000**, *45*, 1911. [Crossref]

[30] Singh, R. N.; Singh, J. P.; Lal, B.; Thomas, M. J. K.; Bera, S. *Electrochim. Acta* **2006**, *51*, 5515. [Crossref]

[31] Suresh, G. K.; Akbar, J.; Govindan, R.; Girja, E. K.; Kanagraj, M. *J. Sci. Adv. Mat. Devices* **2016**, *1*, 282. [Crossref]

[32] Singh, R. N.; Singh, J. P.; Lal, B.; Singh, A. *Int. J. Hydrogen Energy* **2007**, *32*, 11. [Crossref]

[33] Karakas, Z. K.; Boncukcuoglu, R.; Karakas, I. H.; Ertugru, I. M. *J. Magn. Magn. Mater.* **2015**, 37, 298. [Crossref]